Chemical Science Review and Letters ISSN 2278-6783

Research Article

Water Soluble Non-toxic Organic Zinc Corrosion Inhibitors in Acidic Solution

Omar A. Hazazi*

Chemistry Department, Faculty of Applied Sciences, Umm Al-Qura University, Makkah Al-Mukarramah, Saudi Arabia Kingdom

Abstract

The corrosion inhibition of Zn was investigated in acidic solutions using some polysorbate compounds (tweens) as environmentally safe corrosion inhibitors. The corrosion rate was calculated in the absence and presence of the corrosion inhibitor using various techniques. The corrosion inhibition process was found to depend on the adsorption of the tween molecules on the metal surface as supported by their influence on the ethanol oxidation at Pt electrode using cyclic voltammetric technique. Electrochemical measurements indicated that all the additives behave as mixed-type inhibitors. The corrosion inhibition efficiency was found to depend on the concentration of the tween and its structure.

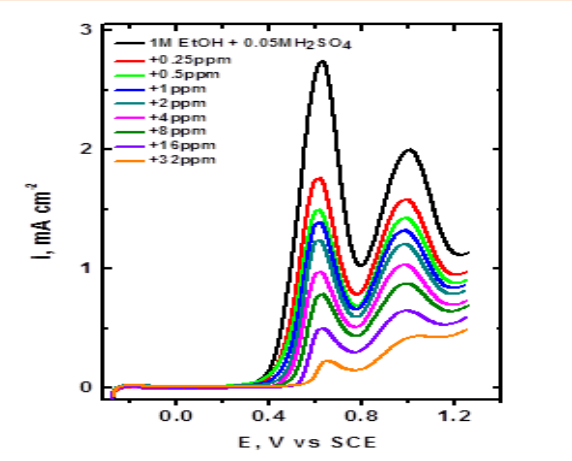

Keywords: Zinc, EIS, polarization, cyclic voltammetry, Acid corrosion, Tween

***Correspondence**
Author: Omar A. Hazazi
Email: oahazazi@hotmail.com

Introduction

Zinc is an active metal with numerous industrial applications. Metallic zinc is used in the production of alloys, as a favorable anode for primary dry batteries [1] and in galvanizing to protect steel structures [2]. However, as reactive metal it suffers from high corrosion rate in contact with various media, specially the acidic one. Addition of inhibitor materials is one of a possible way to control its corrosion rate.

A variety of inorganic and organic compounds have been reported as corrosion inhibitor. In spite of the inhibition efficiency of additive on the corrosion rate, two mean key factors have limit the use of inhibitors in practical applications. On one hand the limitation of the inhibitors' solubility in aqueous media. This reduces the numbers of available compounds to some groups like amino acids [3] and quaternary salts [4, 5]. On the other hand, the toxicity of most available inhibitors, even water soluble compounds, limits their use due to the environmental threat.

Natural products of plant origins as well as some nontoxic organic compounds, which contain polar functions with nitrogen, oxygen and/or sulfur in conjugated systems in their molecules, have shown encouraging results when used as corrosion inhibitors in many corrosion systems [6–23]. However, one of the major problems associated with the use of natural products as corrosion inhibitors, is the isolation and characterization of the active constituents responsible for the inhibition process. In the light of this, the present study seeks to investigate the possibility of using a series of tween compounds as inhibitors for zinc in acidic media. Tween compounds are a nonionic surfactants soluble in water and often used as emulsifier in food and pharmaceutical application [24, 25] due to their non-toxicity.

Experimental

Materials

All solutions were prepared from bidistilled water and analytical grade chemicals H_2SO_4 (BDH), tweens compounds (BDH), shown as **Figure 1**, and ethanol (Merck). Inhibitor stock solutions were prepared in ethanol–water mixture.

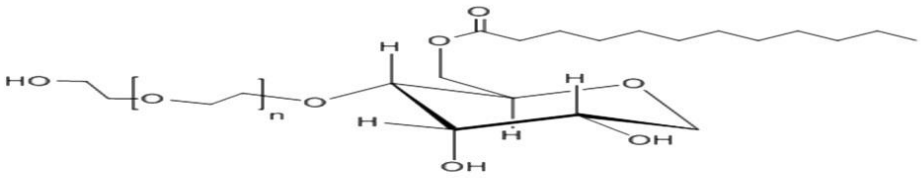

Compound (I) Tween-20(polyoxyethylene sorbitan monolaurate).

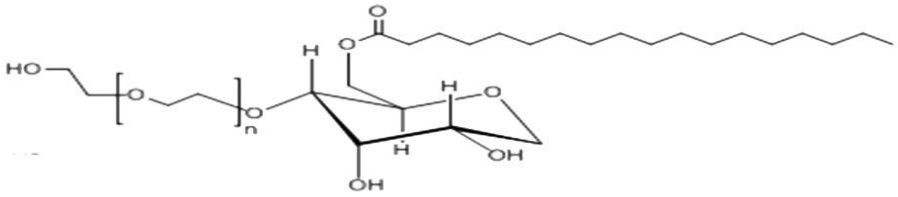

Compound (II) Tween-60(polyoxyethylene sorbitan monostearate).

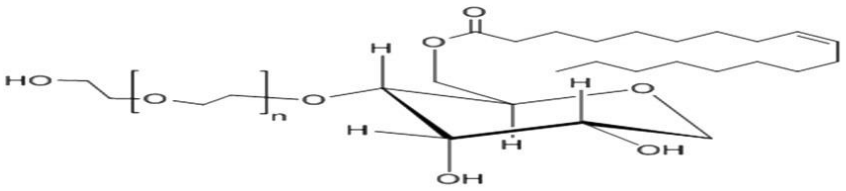

Compound (III) Tween-80(polyoxyethylene sorbitan monooleate).

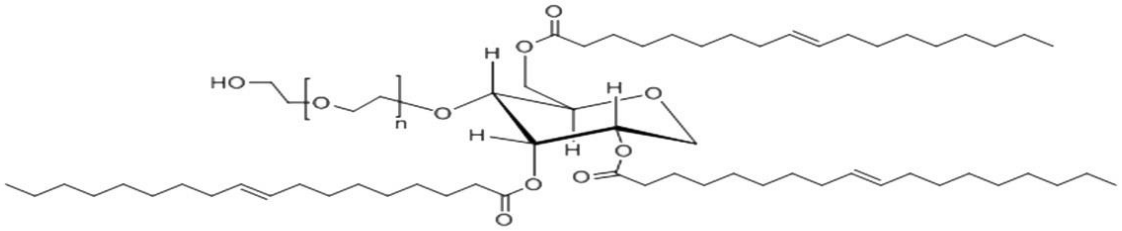

Compound (IV) Tween-85(polyoxyethylene sorbitan trioleate)

Figure 1 Stereochemistry of tween compounds.

The working electrodes for potentiodynamic curves and EIS measurements were prepared from Zinc rod (Aldrich 99.99%) sealed with epoxy resin so that only cross section of (0.71cm^2) of the rod was exposed. The surface preparation of the specimens was carried out using emery papers of different grades down to 1200, ultrasonically degreased for 5 min with acetone and rinsed with bi- distilled water [26]. Pt sheet and a saturated calomel electrode (SCE) were served as counter and reference electrodes, respectively.

Apparatus

Weight-loss measurements were conducted by suspending the coupons in a 150 mL vessel placed in a thermostat water bath. Electrochemical measurements were performed in one compartment three-electrode cell using ACM Instruments (Gill AC serial no. 1258), operated under full computer control to obtain the polarization curves and electrochemical impedance spectra.

Procedure

All experiments were undertaken in stagnant aerated solution. The oxygen content of the solution was limited to that from natural aeration.

Weight loss measurements

The Zinc specimens (rectangular in the form 2 x 2 x 0.1 cm) were grinded with emery paper of different grades down to 1200, washed, ultrasonically degreased for 5 min with acetone and rinsed bi-distilled water, dried and weighed. The coupons with freshly prepared surfaces were then fully immersed in quiescent test solutions for 4 days at the required temperature. Each experiment was carried out twice and then the processed sample was removed, washed, dried and reweighed.

Potentiodynamic polarization measurements

The degreased working electrodes were inserted into the solution. After 20 min. of immersion, the zinc electrode was then polarized. The current-potential curves were obtained by changing the electrode potential automatically from -200 to +200 mV with scan rate 20 mV/min.

*Electrochemical impedance spectroscopy***:** The EIS experiment was performed at open circuit potential (E_{OC}) over a frequency range of 10 kHz to 100 mHz. The sinusoidal potential perturbation was 10 mV in amplitude.

Cyclic voltammetry

For cyclic voltammetry measurements, Pyrex glass three compartment cell equipped with Pt sheet as a working electrode has been used. The experiments were performed according to the following procedure with scan rate 100 mV/s:

- The Pt electrode was activated in 0.05 M H_2SO_4 by repetitive triangular sweep while changing the electrolyte repeatedly until the voltammogram acquired its usual shape as shown in **Figure 2**.
- The electrolyte was replaced by 0.05 M H_2SO_4 in the presence of 1M ethanol and the steady voltammogram was recorded.
- The required amount of the tween was introduced to the cell and the voltammogram was recorded after 2 min cycling.

The real surface area of the Pt electrode has been determined from the hydrogen adsorption/desorption charge of the voltammogram recorded in step one taking into account 210 μC/cm^2 of Pt surface [27].

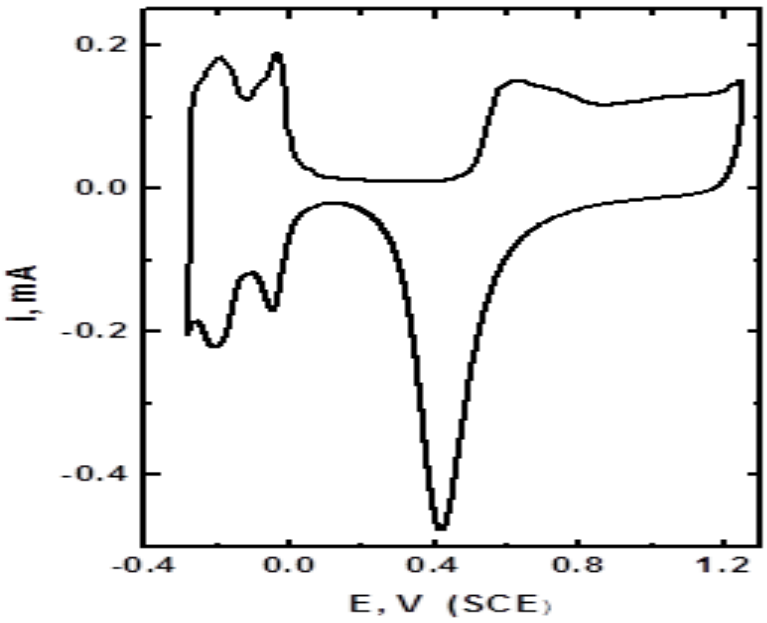

Figure 2 Cyclic voltammogram of Pt electrode in 0.05 M H_2SO_4, Scan rate =100 mV/s and at 30°C

Results and Discussion

Weight loss technique

Influence of inhibitor nature and concentration: In general, the efficiency of an organic substance as an inhibitor for metallic corrosion depends on the structure of the inhibitor, nature of the metal and the other experimental conditions, such as concentration of inhibitor, temperature, pH of the electrolyte …. etc. In order to study the influence of these factors on zinc corrosion, the data obtained from weight loss measurements for all additives are collected in **Figure 3**. These curves indicate that corrosion rate depends on the structure and concentration of the compounds under investigation.

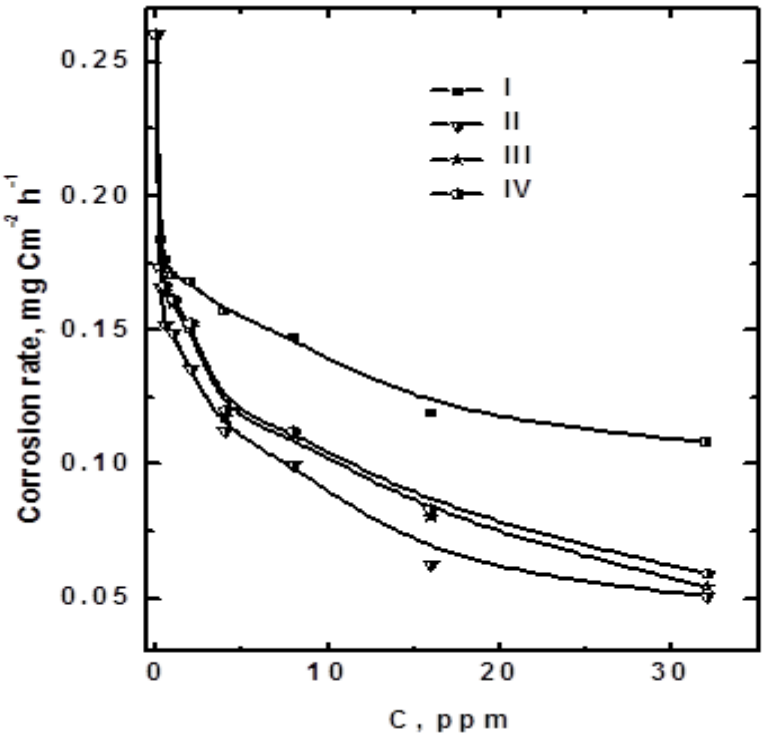

Figure 3 Plot of corrosion rate against inhibitor concentrations for zinc in 0.05 M H_2SO_4 at 30°C.

Adsorption isotherm

A theoretical fit of the data to the Freundlish adsorption isotherm (Eq. (1)) and to the recent kinetic-thermodynamic model [28, 29] (Eq. (2)) for all inhibitors is given in **Figures 4** and **5**.

$$\log \theta = \log k + n \log C \quad (1)$$

$$\log \left(\frac{\theta}{1-\theta} \right) = \log k' + y \log C \quad (2)$$

Where, K is the equilibrium constant of the adsorption reaction, C is the inhibitor concentration in the bulk of solution, θ is the fraction of the surface occupied by the inhibitor, $0 < n < 1$ and y is the number of inhibitor molecules occupying one active site. The data depicted in Figures 4 and 5, clearly show that excellent fit is obtained with both types of plot.

The change of the free energy ΔG_{ads} is calculated using equation (3), together with the values of $1/y$ and $1/n$ are collected in **Table 1**.

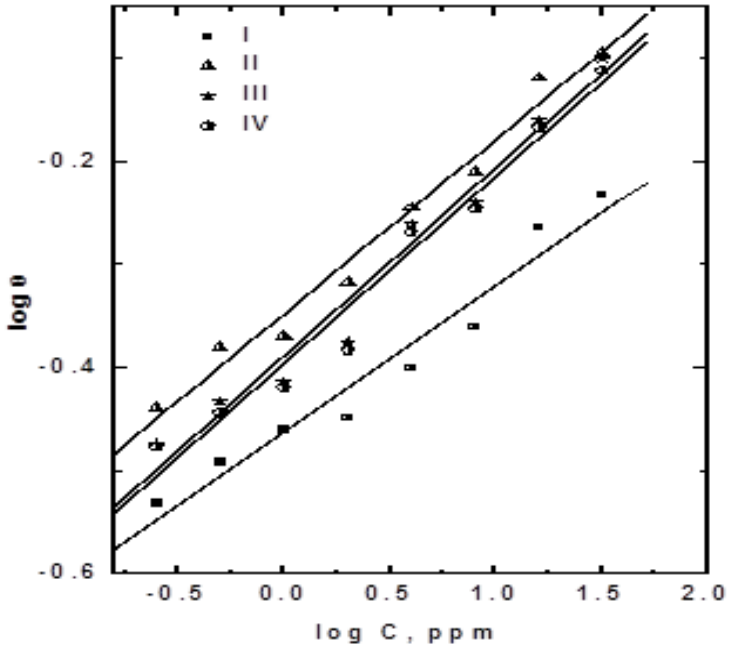

Figure 4 Curve fitting of compound II adsorption by Freundlich isotherm.

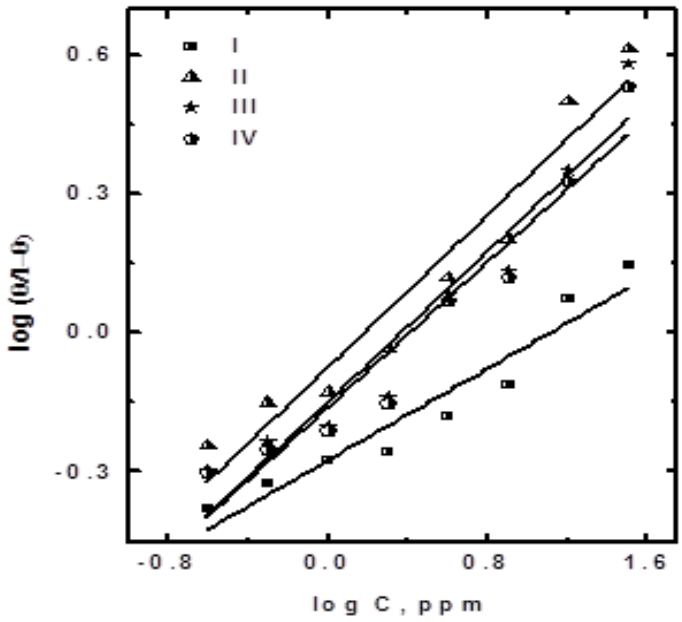

Figure 5 Comparison between the experimental adsorption isotherms (symbols) for tween compounds in the system Zn/0.05M H_2SO_4, x ppm tween and the theoretical kinetic model (—).

Table 1 Inhibitor binding constants (*K*), free energy of binding ($\Delta G_{ads.}$, $kJmol^{-1}$) and number of active sites (1/y&1/n) for tween at 30°C .

Inhibitors	Kinetic model		Freundlich isotherm	
	1/y	$-\Delta G_{ads.}$(KJ mole^{-1})	1/*n*	$-\Delta G_{ads.}$ (KJ mole^{-1})
I	4.032	3.68	7.071	7.43
II	2.433	10.11	5.914	8.10
III	2.421	7.91	5.650	7.85
IV	2.591	7.83	5.364	7.83

$$K = \frac{1}{55.5} \exp(-\Delta G_{ads}/RT) \quad (3)$$

Values of 1/*y* and *1/n* greater than unity indicate that a given inhibitor molecule will occupy more than one active site [28, 30]. It is well known that values of ΔG_{ads} in the order of -20 KJ mole^{-1} or lower indicate a physisorption, those about -40 KJ mole^{-1} or higher involve charge sharing to form a coordinate type bond [31]. This indicates that tween compounds adsorption takes place through electrostatic interaction between the inhibitor molecule and the zinc surface. The negative value of ΔG_{ads}, reveals a spontaneous adsorption process. As can be seen from Table 1, the values of ΔG_{ads} show that the order in which the efficiency of the investigated compounds decreases can be written as II > III > IV>I.

Effect of temperature

The influence of temperature on the corrosion rate of Zinc in 0.05M H_2SO_4 in the absence and presence of different concentration of additives was investigated by weight loss technique in the temperature range (30 to 60°C). The corrosion rate of zinc with or without tween compounds was found to increase with increasing the solution temperature. The decrease in corrosion inhibition may due to the desorption of the molecules from the surface of the Zinc by increasing the temperature. This indicates that the inhibitor is physically adsorbed on Zn surface. This suggests that the adsorbed molecules mechanically screen the coated part of the metal surface from the action of the corrodent.

Thermodynamics parameters

On the basis of Arrhenius-type equation

$$K = A \exp(-E_a^*/RT) \quad (4)$$

Activation energy, E_a^*, can be obtained from the slope of the linear relationship between the logarithm of corrosion rate (log *k*), and the reciprocal of absolute temperature (1/*T*) (**Figure 6**).

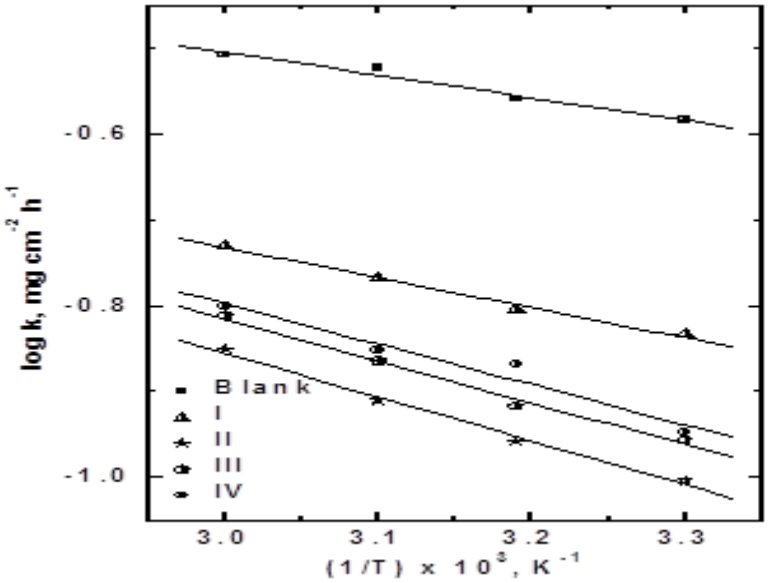

Figure 6 Arrhenius plots for zinc electrode in 0.05 M H_2SO_4 in the absence and presence of 8 ppm of tweens.

In all cases studied, a plot of log (corrosion rate/*T*) vs. (1/*T*) resulted in straight lines with a slope -ΔH*/2.303*R* and intercept of [log (*R*/*Nh* + Δ*S**/2.303 *R*) according to the transition state equation (Eq.5). (please physical constants in the below Eq. and all equations should be in italic)

$$K = \frac{RT}{Nh} \exp(\Delta S^*/R)\exp-(\Delta H^*/RT) \quad (5)$$

Typical plots are shown in **Figure 7** and all calculated thermodynamics parameters for blank solution and 8 ppm additives are given in **Table 2**. Data given in Table 2 revealed that the inhibitive additives cause an increase in the activation energy value, as compared with the blank solution which could be interpreted by physical adsorption [32]. The positive signs of ΔH^* reflect the endothermic nature of the zinc dissolution process. Large and negative values of ΔS^* imply that the activated complex in the rate-determining step represents an association rather than dissociation step, meaning that decrease in disordering takes place on going from reactants to the activated complex [33].

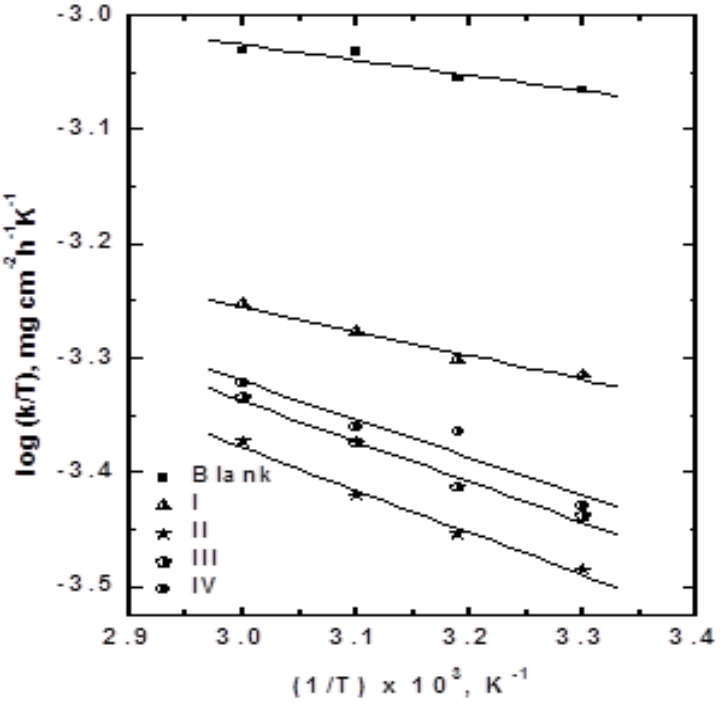

Figure 7 Plots log (k / T) vs. 1/T) for zinc in 0.05 M H_2SO_4 in the absence and presence of 8 ppm of inhibitors.

Table 2 Thermodynamic activation parameters for dissolution of zinc in 0.05 M H_2SO_4 in the absence and presence of 8 ppm of inhibitors, after 4 days at 30°C

Inhibitors	E_A* (KJ mole^{-1})	ΔH^* (KJ mole^{-1})	$-\Delta S^*$ (J mole^{-1} K^{-1})
0.0	5.00	2.43	249.31
I	6.71	4.07	247.69
II	9.78	7.15	240.82
III	9.38	6.74	241.26
IV	9.00	6.37	242.06

Polarization measurements

To elucidate the influence of the change of the molecular structure of investigated tweens on the corrosion of Zn in sulfuric acid, the potentiodynamic ***I*(*E*)** curves of 8 ppm of all tweens investigated are presented in **Figure 8.** For comparison, the voltammogram of the uninhibited solution is also included. The main information obtained from the difference between the voltammograms recorded with and without inhibitors in solution is related to the current density variation in the whole potential range. These show that the order in which the current density decreases relative to the change in molecular structure of the inhibitors is similar to that obtained from weight loss measurements.

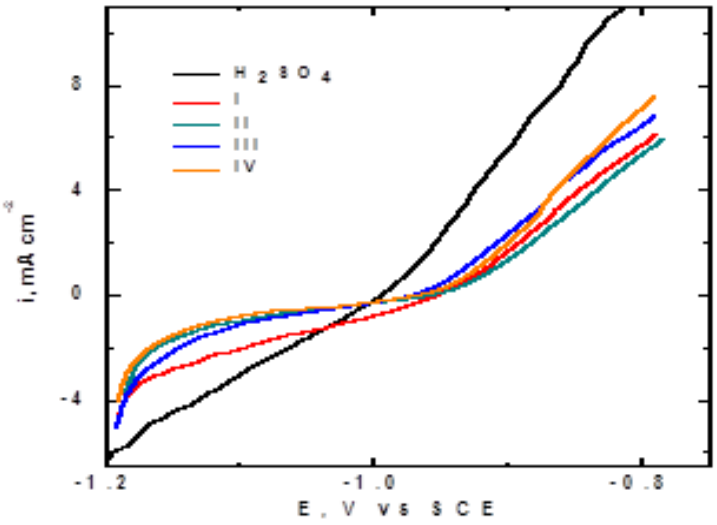

Figure 8 Potentiodynamic polarization curves of Zn in 0.05 M H_2SO_4 in the absence and presence 8 ppm of tweens, scan rate =20 mV/min.

Based on this data, Tafel plot (**Figure 9**) for Zn corrosion in 0.05 M H_2SO_4 in the absence and presence of different concentrations of compound (II) has been drawn. It can be seen from this Figure that the increase of compound (II) concentration from 0.25 ppm to 32 ppm resulted in depression of polarization curves. Bothe the anodic and cathodic current densities were decreased in Figure 9 indicating that tween suppressed both the anodic and cathodic reactions through adsorption on the zinc surface. This suggests that tween act as mixed-type corrosion inhibitor for zinc in 0.05 M H_2SO_4 solution.

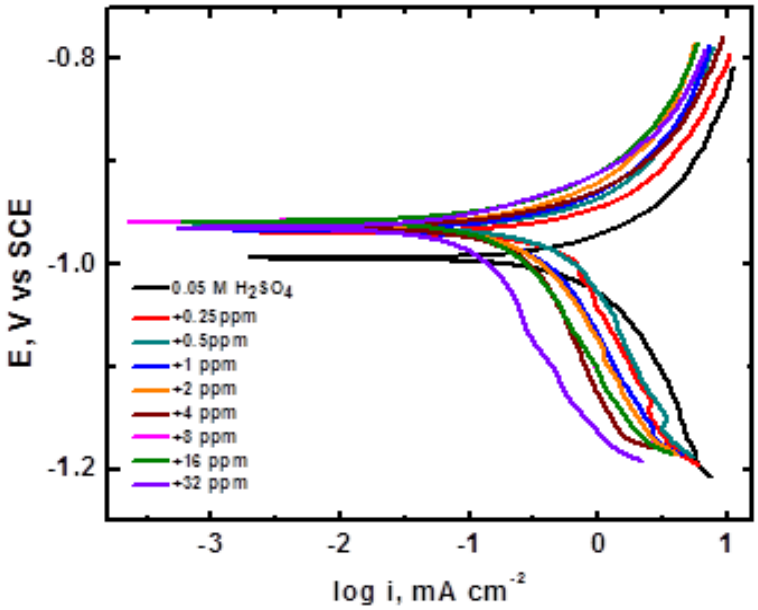

Figure 9 Tafel plots for Zn in 0.05M H_2SO_4 in the absence and presence of various concentration of compound II.

The corrosion parameters estimated from slopes and intercept of cathodic and anodic Tafel lines are listed in **Table 3**. The experimental data show that the corrosion current density (I_{corr}) decreased as the concentration of inhibitors increased. The Tafel slopes $ß_c$ and $ß_a$, remain unchanged, indicating that the retardation of the reactions (metal dissolution and hydrogen evolution) was retarded without changing the mechanism, i.e., the adsorbed molecules mechanically screen the coated part of the electrode and therefore protect it from the action of the corrosive medium. To find out the influence of changes in the molecular structure of the investigated compounds on the

protection efficiency, the protection efficiency (P_i) obtained from polarization curves of 8 ppm concentration of all the additives investigated are collected in **Table 4**. These show that the order in which the protection efficiency decreases relative to a change in a molecular structure of the additives is similar to that obtained from other techniques.

Table 3 The effect of compound (II) concentration on Zn dissolution in 0.05M H_2SO_4 at 30°C

Concentration (ppm)	$E_{corr.}$ (mV)/SCE	$i_{corr.}$(mA cm^{-2})	Tafel slope (mV/current decade)		P_i
			β_a	β_c	
0	1008.4	1.452	0.173	0.264	-
0.25	996.7	0.706	0.147	0.248	51.31
0.5	993.9	0.597	0.132	0.231	58.83
1	989.7	0.425	0.137	0.215	70.69
2	986.3	0.36	0.144	0.246	75.17
4	984	0.332	0.129	0.217	77.1
8	982.7	0.189	0.109	0.195	86.97
16	982.5	0.16	0.112	0.176	88.97
32	980.2	0.09	0.1	0.179	93.79

Table 4 Protection efficiency as determined by polarization technique for all compounds under investigation at 8 ppm in 0.05M H_2SO_4 at 30°C.

Compound	P_i
I	71.93
II	86.97
III	78.97
IV	78.62

Electrochemical impedance spectroscopy (EIS)

EIS diagrams obtained in the presence of compound (II) (what is compound II) at the different concentrations in 0.05M H_2SO_4 are shown in **Figure 10**. Visual inspection of EIS spectra and analysis of the results with equivalent circuit provides useful interpretation of inhibition performance of tween in 0.05M H_2SO_4 solution.

Phase angle at high frequencies provides a general idea of anticorrosion performance. The more negative the phase angle the more capacitive the electrochemical behavior [34]. Charge transfer resistance increment could raise current tendency to pass through the capacitor in the circuit. According to appearance of theta vs. frequency diagrams, increasing the concentration of tween in the test solutions results in more negative values of phase angle at high frequencies indicating superior inhibitive behavior at higher concentrations. The increase of absolute impedance at low frequencies in Bode plot confirms the higher protection with increasing the concentration of inhibitors, which is related to adsorption of inhibitors on zinc surface. The recorded EIS spectra show one depressed capacitive loop for each measurement. Deviation of the capacitive loop from a perfect semi circle could be attributed to heterogeneity of the surface. **Figure 11** depicts typical fitting results of EIS diagrams with the provided equivalent circuits, where R_s represents solution resistance, R_{ct} charge transfer resistance and C_{dl} the double layer capacitance.

The best-fit parameters are shown in **Table 5**. The capacitance values were calculated according to the following equation

$$C_{dl} = \frac{1}{2\pi} f_{max} R_{ct} \qquad (6)$$

Where f_{rnax} is the maximum frequency.

Protection efficiency (P_i) of the investigated inhibitors can be calculated using equation 7.

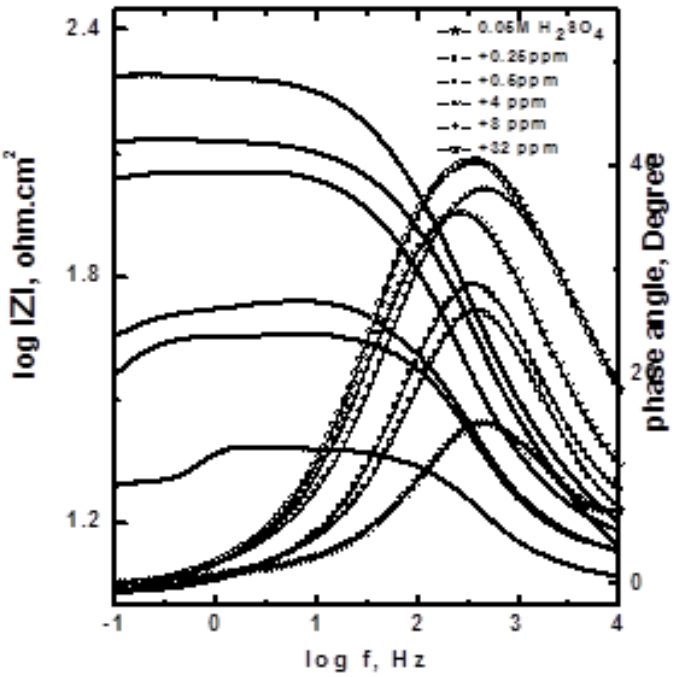

Figure 10 Bode diagrams for Zn in 0.05M H_2SO_4 containing different concentrations of compound II

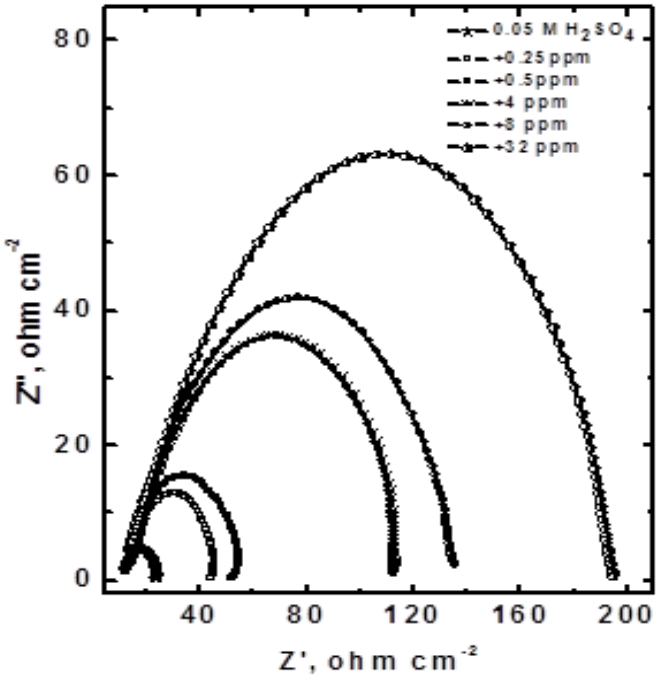

Figure 11 Comparison of experimental impedance measured for zinc immersed in 0.05M H_2SO_4 in the absence and presence 8ppm tweens (symbols) with that obtained using the provided equivalent circuit (solid line).

$$P_i = \frac{R_{ct} - R^{\circ}_{ct}}{R_{ct}} \times 100 \qquad (7)$$

Where R°_{ct} and Rct are the charge transfer resistances in the absence and presence of inhibitor, respectively. It can be seen from Table 5 that the values of R_{ct} increase with the increasing of the inhibitor concentration [35-37]. It is also

noted that the C_{dl} values tend to decrease when the concentration of inhibitor increases. This decrease in C_{dl}, which can result from a decrease in local dielectric constant and/or an increase in the thickness of the electrical double layer [38], suggests that these compounds molecules function by adsorption at the metal/solution interface.

The protection efficiency (P_i) of the investigated compounds as obtained from electromechanical impedance measurements (**Table 6**) were found to decrease according to the following order: compound (II) > compound (III) > compound (IV)> compound (I)

Table 5 Electrochemical kinetic parameters by EIS technique for the corrosion of zinc in 0.05 M H_2SO_4 at different concentrations of compound II at 30°C.

Compound	Conc.(ppm)	C_{dl} (µF cm^{-2})	R_{ct} (Ohm cm^2)	θ	P_i
II	0.25	113.3	33.2	0.596	59.61
	0.5	100.8	43.9	0.694	69.36
	1	95.9	51.7	0.741	74.06
	2	84.8	91.1	0.853	85.28
	4	73.7	105.5	0.873	87.29
	8	69.5	123	0.891	89.11
	16	55.9	127.4	0.895	89.48
	32	39.2	182.8	0.922	92.23

Table 6 Protection efficiency as determined by EIS technique for all compounds under investigation at 8 ppm in 0.05M H_2SO_4 at 30°C.

Compound	P_i
I	69.44
II	89.11
III	85.16
IV	84.99

Cyclic voltammetric study

In order to verify the idea that the inhibition of Zn corrosion by compounds under investigation is due to their adsorption on the electrode surface, which leads to screen its surface from the aggressive SO_4^{2-} ions. We studied the influence of their adsorption at Pt surface on the ethanol oxidation in H_2SO_4 solution using cyclic votammetric technique. The results obtained for compound II is shown in **Figure 12**. It is clearly observed from this Figure that the adsorption of compound II leads to a marked decrease in the ethanol oxidation peaks. This effect becomes more pronounced as its concentration increases. The other additives exhibit a similar behavior. In addition to that, addition of tween compounds lead to the shift of onset of ethanol oxidation potential. Which indicates that the oxidation of ethanol was delayed until some Pt surface site becomes free from adsorbed tween compounds. This is an additional evidence for the stability of the adsorbed tween compounds at Pt surface. Moreover, this shift in the onset ethanol oxidation potential was found to increase with additive concentration. This clarify that the adsorption properties of tween compounds depends on its concentration in aggrieves media.

In order to find out the order of adsorption capability of these compounds, a ratio between the oxidation current peaks in absence (i_p) and presence of additives, $i_{p,add}$, for the peak located at 0.625 ± 0.02V/SCE, has been taken as a measure. It is clearly from **Figure 13** that the adsorption capability of the studied compounds on the Pt surface decreases in the following order:

Compound (II) > compound (III) > compound (IV)> compound (I)

This result is in a good agreement with corrosion inhibition data obtained by other techniques.

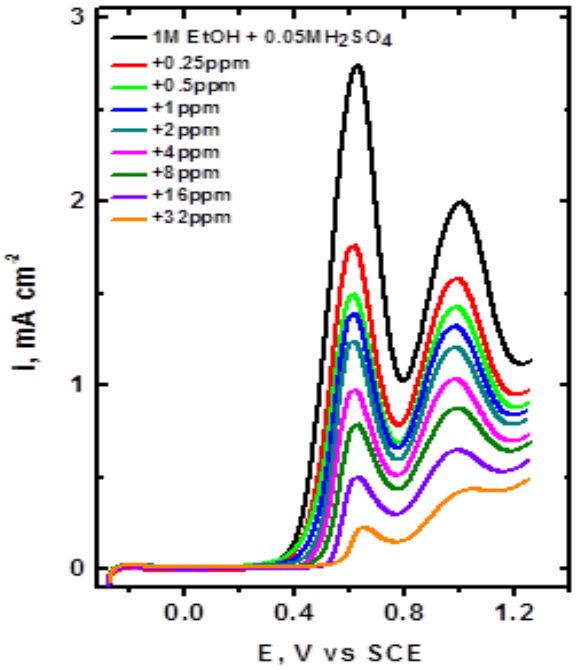

Figure 12 Anodic sweep voltammograms for ethanol oxidation in 0.05 M H_2SO_4 + 1 M ethanol in the absence and presence of different concentrations of compound II at 30°C.

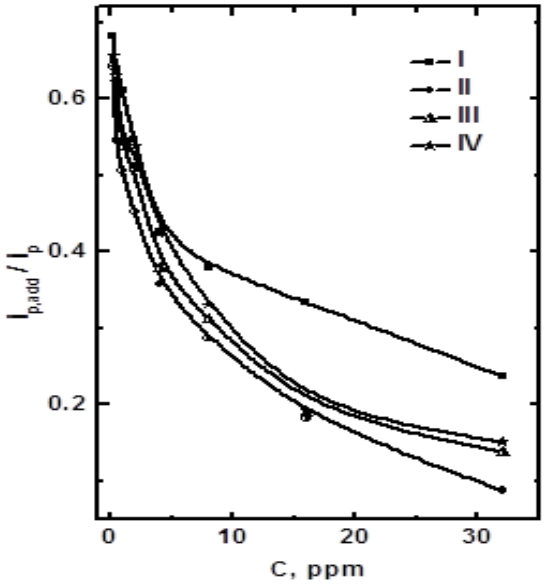

Figure 13 Plot of the current peak ratio for ethanol oxidation vs. inhibitor concentration at 30°C.

Mechanism of corrosion inhibition

Tween compounds are basically polyoxyethelene sorbitan combined with different fatty acids. The number associated with the tween name determines the predominant fatty acid contained in the tween structure. Thus, for tween 20, 60, 80 and 85, the acids are monolaurate, monostearate ,monooleate and trioleate, respectively. The extent of inhibition of different tween compounds (shown in Figure 1) depends on their structures. Figure 1 shows the stereochemistry of tween compounds under investigation. From all the techniques used in this work the inhibition efficiency decreases in the following order:

T - 60 >T - 80 > T- 85 > T – 20

These better performances can be explained as follows. The tween compounds have the same hydrophilic part, CHO $(CH_2CH_2O)n$ CH_2CH_2OH, attaches to the zinc surface, while the different hydrophobic part. Consequently, the difference of inhibition could be attributed to the difference in the hydrophobic part which is one group of $(CH_2)_{10}CH_3$, one group of $(CH_2)_{16}CH_3$, one group of $(CH_2)_7CH(C_8H_{17})CH_3$ and three groups of $(CH_2)_7CH(C_8H_{17})CH_3$ for tween-20, tween-60, tween-80 and tween-85, respectively. These parts extend to the solution bulk. Consequently, the effectiveness of surfactant as corrosion inhibitor depends on the hydrophobic carbon chain, and it is generally accepted that the augmentations of the hydrophobic hydrocarbon chain length often raise the protection effect [39-42]. Possibly for the following reasons: (i) the thickness of hydrophobic barrier layer increases with the carbon chain length, which has more screening effect on acidic media. Namely, it is difficult for H_2 and Zn^{2+} to diffuse owing to the thicker hydrophobic layer. (ii) Adsorption of tweens may occur through the hetero-oxygen atom. The hydrophobic alkyl has negative inductive effect. So, the electron density at the oxygen atom will increases with the hydrophobic carbon chain length. Hence, this will stabilize the interaction between Zn and O(tween) and therefore will raise the protection efficiency [39]. Thus, tween-20 exhibited the lowest protection efficiency as it has the shortest hydrophobic group $[(CH_2)_{10}CH_3]$. Tween-60 and tween-80 contain the same number of carbon atoms in the hydrophobic part. One can expect that tween-80 should give higher inhibition [40] than tween-60 due to the presence of double bond in the former. However, according to our result, tween-60 exhibited higher inhibition efficiency. This may be attributed to the restricted conformation of tween-80 by cis - form of this double-bond. However, tween-85 has three hydrophobic groups $[(CH_2)_7CH(C_8H_{17})CH_3]$, its protection efficiency is lower than both tween 60 and 80. This can be attributed to the prominent steric hindrance effect of the three hydrophobic groups which make it difficult to reach saturation of the zinc surface.

Conclusions

- Evaluation of polarization measurements revealed that these compounds suppress cathodic and anodic polarization curves, and they behave as the mixed type corrosion inhibitors
- EIS measurements depicted increase of charge transfer resistance and double layer capacitance in the presence of tween compound confirming adsorption of these molecules on the surface.
- The studied compounds were found to inhibit the ethanol oxidation at the Pt surface via their adsorption.
- Adsorption of inhibitors molecules on the Zn surface was found to obey both Freundlish isotherm and the kinetic thermodynamic model.
- The inhibition efficiency was found to be related to the chemical structure and depend mainly upon the hydrocarbon side chain in these compounds i.e. the hydrophobic part.

References

[1] Ein-Eli Y., Auinat M., Straosvetsky D., J. Power Sources 2003, 114, 330.
[2] Qu Q., Li L., Bai W., Yan C., Cao C., Corr. Sci. 2005, 47, 2832.
[3] Fouda A.S., Madkour L.H., El-Shafei A.A., Abd ElMaksoud S.A., Bull Korean Chem. Soc. 1995, 16, 454.
[4] Abdallah M., El-Etre A.Y., Moustafa M.F., Port. Electrochim. Acta 2009, 27, 615.
[5] Mihit M., Laarej K., Abou El Makarim H., Bazzi L., Salghi R., Hammouti B., Arabian J. Chem. 2010, 3, 55.
[6] Abdallah M., Zaafarany I., Fouda A.S., Abd El-Kader D., J. Mater. Eng. Perform. Pub;ished online: 02 July 2011.
[7] Shanbhag A.V., Venkatesha T.V., Prabhu R.A., Praveen B.M., Bull. Mater. Sci. 2011, 34, 571.
[8] El-Shafei A.A., Moussa M.N.H., El-Far A.A., J.Appl.Electrochem. 1997, 27, 1075.
[9] El-Shafei A.A., Moussa M.N.H., El-Far A.A., Mater. Chem. Phys. 2001, 70, 175.
[10] Moussa M.N.H., El-Far A.A., El-Shafei A.A., Mater. Chem. Phys. 2007, 105, 105.
[11] Feng Y., Siow K.S., Teo W.K., Hsieh A.K., Corros. Sci. 1999, 41, 829.
[12] Morad M.S., El-Hagag A., Hermas A., Abdel Aal M.S., J. Chem. Technol. Biotechnol. 2002, 77, 486.
[13] Zhang D.Q., Gao L.X., Zhou G.D., J. Appl. Electrochem. 2003, 33, 361.
[14] Oguzie E.E., Unaegbu C., Ogukwe C.N., Okolue B.N., Onuchukwu A.I., Mater.Chem. Phys. 2004, 84, 363.
[15] Moretti G., Guidi F., Grion G., Corros. Sci. 2004, 46, 387.

[16] Li Y., Zhao P., Liang Q., Hou B., Appl. Surf. Sci. 2005, 252, 1245.
[17] Shibli S.M.A., Saji V.S., Corros. Sci. 2005, 47, 2213.
[18] Mu G., Li X., J. Colloid Interface Sci. 2005,289, 184.
[19] Badawy W.A., Ismail K.M., Fathi A.M., J. Appl. Electrochem. 2005, 35, 879.
[20] Oguzie E.E., Mater. Chem. Phys. 2006, 99, 441.
[21] Badawy W.A., Ismail K.M., Fathi A.M., Electrochim. Acta 2006, 51, 4182.
[22] Oliveres O., Likhanova N.V., Gomez B., Navarrete J., Lianos-Serrano M.E., Arce E., Hallen J.M., Appl. Surf. Sci. 2006, 252, 2894.
[23] Eddy N.O., Green Chem. Lett. Rev. 2010, 3, 307.
[24] Rao J., McClements D.J., Food Hydrocolloids 2012, 26, 268e.
[25] Koocheki S., Madaeni S.S., Niroomandi P., Saudi Pharmaceutical Journal 2011, 19, 255.
[26] Foad El Sherbini E.E., Abd El Rehim S.S., Corros. Sci. 2000, 42, 785.
[27] Biegler T., Rand D.A.J., Wood R., J. Electroanal. Chem. 1971, 29, 269.
[28] El-Awady A., Abd El-Nabey B., Aziz G., J. Electrochem. Soc. 1992, 139, 2150.
[29] El-Awady A., Abd El-Nabey B., Aziz S., Khalifa M., Al-Ghamedy H., Int. J. Chem. 1990, 1, 169.
[30] Shams El-Din A.M., Moussa M.N.H., El-Sum E.A., Proceedings of the 11th International Corrosion Congress, Florence, Italy, 1990.
[31] Küstü C., Emregül K.C., Atakol O., Corros. Sci. 2007, 49, 2800.
[32] Vracar L.M., Drazic D.M., Corros. Sci. 2002, 44, 1669.
[33] Gomma M.K. and Wahdan M.H., Mater. Chem. Phys. 1995, 39, 209.
[34] Mahdavian M., Attar M.M., Corros. Sci. 2006, 48, 4152.
[35] Hassan H.H., App. Surf. Sci. 2001, 174, 201.
[36] Bentiss F., Traisnel M., Lagrenee M., Corros. Sci. 2000, 42, 127.
[37] M. G. Hosseini, Electrochim. Acta 2007, 52, 3650.
[38] El-Shafei A.A., Abd El-Maksoud S.A., Fouda A.S., Corros. Sci. 2004, 46, 579.
[39] Foad El-Sherbini E.E., Abdel Wahaab S.M., Deyab M., Mater. Chem. Phys. 2005, 89, 183.
[40] Abdallah M., El- Etrre A. Y., Port. Electrochim. Acta 2003, 21, 315.
[41] Elachouri M., Hajji M. S., Salem M., Kertit S., Coudert R., Essassi E. M., Corros. Sci. 1995, 37, 381.
[42] Osman M. M., Shalaby M. N., Anti-Corros. Methods Mater. 1997, 44, 318.

Publication History
Received 26th Aug 2015
Revised 15th Sep 2015
Accepted 07th Oct 2015
Online 30th Oct 2015